Diffusion of Macromolecules in Collagen and Hyaluronic Acid, Rigid-Rod–Flexible Polymer, Composite Matrices

V. Shenoy and J. Rosenblatt*

Collagen Corporation, 2500 Faber Place, Palo Alto, California 94303

Received November 11, 1994; Revised Manuscript Received September 19, 1995®

ABSTRACT: Diffusivities of bovine serum albumin and dextran were measured in matrices of concentrated succinylated collagen (SC), a rigid-rod biopolymer, and hyaluronic acid (HA), a more flexible biopolymer. The diffusional behavior was found to be influenced by the rigidity of the matrix polymer chain as well as by the rigidity and morphology of the diffusing solute. Matrices composed of mixtures of SC and HA showed more diffusional hindrance than matrices comprised of only SC or HA. The diffusional hindrance varied depending on the composition of the matrix (i.e., ratio of rigid-rod to flexible polymer). Electron spin resonance studies using spin-labeled high molecular weight flexible probes indicate that the rigid-rod SC molecules are able to mix with the flexible chains. The apparent interpenetration of the flexible chains (HA) within the rigid-rod (SC) matrix submesh reduces the mesh size in the composite matrix as well as increases the rigidity of the flexible chain.

Introduction

Diffusion of polymer solutes in concentrated biopolymer matrices is important in many biomedical and biochemical applications. The transport process has a direct impact in applications including size-exclusion chromatography, membrane permeation, and controlled drug release. This study had a practical goal of studying diffusion in injectable biopolymer matrices for controlled delivery of polypeptide drugs. A controlled-release matrix forms a reservoir of drug from which the drug is released at a controlled rate over a long period of time.[1] The large size and susceptibility to enzymatic degradation of many therapeutic polypeptides[2] precludes their administration by more traditional oral and transdermal routes. Hence, the most practical near-term route for controlled delivery of these drugs is through parenteral administration (dosage forms which are either injected or surgically implanted under the skin).[3] The choice of collagen and hyaluronic acid (HA) as matrix polymers was based on their availability in highly purified forms and their established biocompatibility.[4,5] The diffusional measurements in these matrices were performed using fluorescently labeled bovine serum albumin (BSA) and dextran. Since collagen and BSA are rigid, and HA and dextran are more flexible, some fundamental insights into the role of polymer rigidity in the diffusional behavior of macromolecules in concentrated biopolymer matrices can be obtained from this study.

Collagen is a naturally occurring structural protein (MW 300 kDa). The tightly wound triple-helical structure of collagen[6] makes it behave like an inelastic rigid rod in solution, thereby distinguishing it from most other biopolymers, which are more flexible. Collagen, at neutral pH, phase separates to form a liquid crystalline phase (LCP) of highly oriented collagen molecules.[7] The phase separation of collagen can be prevented by derivatizing the molecule to have a net charge at neutral pH. The collagen used in this study was derivatized (succinylated) to have a net negative charge at neutral pH. During the course of this study, matrices of succinylated collagen (SC) only, and HA only, as well as composite matrices of mixtures of SC and HA were investigated. Phase stability calculations have revealed that under most conditions mixtures of rigid-rod and flexible-chain molecules are entropically driven to form two phases (isotropic and anisotropic).[8] The isotropic phase typically accommodates a very low concentration of rigid rods, while the anisotropic phase contains a vanishing concentration of flexible chains. Theoretical studies of concentrated solutions of rigid rods[9] indicate that repulsive energetic interactions between the molecules can result in the anisotropic phase having a high disorientation index (Table 1, ref 9) and a volume fraction comparable to the isotropic phase (Figure 5, ref 9). For the case of SC (net negative charge at neutral pH) and HA (very long chains), electrostatic repulsive interactions between the SC molecules inhibit the close packing and alignment required for formation of a tightly packed anisotropic phase, allowing the possibility of mixing of the dissimilar polymer components.

The diffusivities of model macromolecules in the matrices were calculated from measurements of their release profiles (mass released versus time) into an infinite-sink buffer. The release measurements indicated that diffusivities were reduced relative to their free solution values. The extent of diffusional hindrance was influenced by the rigidity of the matrix polymer as well as by the rigidity of the diffuser. Furthermore, the composite (SC and HA) matrices provided greater diffusional hindrance than matrices (with the same total polymer mass) composed of SC or HA only. To obtain a better understanding of this synergistic behavior, electron spin resonance (ESR) measurements were performed using two different sets of spin probes. Low molecular weight poly(acrylic acid) (PAA) probes (referred to as mesh size probes) labeled with nitroxide spin labels were used to independently estimate the mesh sizes in the composite matrices. The mesh size,[10] which is an average length scale between neighboring polymer chains in the matrix, is the primary determinant of topological constraints toward diffusing molecules. High molecular weight PAA probes (referred to as morphology probes) labeled with nitroxide spin labels were used to elucidate the morphological behavior of flexible polymer chains in the presence of concentrated rigid-rod polymers. Spin-labeled PAA was used as a model high molecular weight flexible chain because of

* To whom correspondence should be addressed.

® Abstract published in *Advance ACS Abstracts,* November 1, 1995.

0024-9297/95/2228-8751$09.00/0

the difficulty of spin-labeling HA. Reduction in the segmental mobility of the labeled polymer chain due to changes in its conformational freedom can be monitored by ESR. Changes in segmental mobility of a flexible chain in the presence of rigid chains (as detected by ESR) would correspond to changes in the morphology of the flexible chain due to interactions with the rigid chain. The morphology of the flexible polymer chain within the rigid-rod network is critical in determining its ability to modulate mesh size. In addition, changes in the segmental mobility of the polymer chain (i.e., loss of flexibility) might also be expected to contribute to diffusional hindrance of large solute molecules. Even though the ESR measurements were performed using high molecular weight PAA morphology probes in the presence of SC and the release measurements were from composite matrices of HA in SC, the interpretation of the morphological behavior of the high molecular weight PAA was assumed to be qualitatively similar to the behavior of any flexible negatively charged polyelectrolyte such as HA in the presence of SC.

Materials and Methods

I. Matrix Preparation. Purified Type I bovine collagen (Collagen Corp., Palo Alto, CA) was succinylated by the procedure of Miyata et al.[11] Purified acidic collagen (pH 2.0) was adjusted to pH 9.0 with 1.0 M NaOH. Succinic anhydride (0.2 mg/mg of collagen) dissolved in acetone (1/20 volume of collagen solution) was added to the collagen solution with stirring. The pH during the addition of succinic anhydride was maintained at 9.0. Stirring was continued for 30 min until the solution turned clear. The pH of the solution was then adjusted to 4.5 with 1.0 M HCl. The succinylated collagen (pI ~ 4.5) which precipitated was then centrifuged and washed repeatedly to remove any unreacted succinic anhydride and acetone. The concentrated precipitate was then suspended in a 20 mM sodium phosphate, 130 mM sodium chloride solution adjusted to pH 7.4 (PBS). Succinylated collagen, due to its net negative charge at neutral pH, does not form fibrils at pH 7. The collagen concentration was then determined by the biuret assay.[12] SC at high concentrations (>20 mg/mL) forms a translucent viscous solution.

Hyaluronic acid (HA), a natural mucopolysaccharide, is a linear flexible polymer which is present in the connective tissues of vertebrates, the synovial fluid of joints, and the vitreous humor of the eye.[13] HA matrices were prepared by dissolving rooster comb hyaluronic acid (Sigma Chemical Co., St. Louis, MO) in PBS. The molecular weight (M_w) of the HA has been previously estimated by light scattering measurements to be approximately 800 kD.[14] Like SC, concentrated HA (>20 mg/mL) forms a translucent viscous solution.

II. Matrix Characterization. Mesh Size Probe Preparation. Probes for mesh size measurements (mesh size probes) were prepared by covalently labeling low molecular weight (M_w 6−31 kDa) poly(acrylic acid) (PAA) (Polysciences, Inc., Warrington, PA) with the spin label 4-amino-2,2,6,6-tetramethylpiperidine 1-oxyl (4-amino-TEMPO) by a dicyclohexylcarbodiimide (DCC) condensation reaction.[15] The labeling density was kept low to prevent dipolar interactions between different spin labels on the probe molecules.[16] The hydrodynamic radii (R_h) of the labeled PAA probes were calculated from free solution diffusion coefficients (D_0) measured by dynamic light scattering. The dynamic light scattering measurements were performed at a scattering angle of 90° with a 4 W argon ion laser (λ = 514 nm) and a Langley Ford Model 1096 correlator. The autocorrelation functions were analyzed using a single-exponent function.

Measurement of mesh sizes in SC and HA matrices (Table 1) by an ESR-based technique has been described previously.[14] The technique is based on monitoring the rotational correlation times of the low molecular weight spin-labeled probes of various sizes in the polymer matrices. As shown in ref 14, the τ_m of the probe as a function of increasing matrix concentration does not change from its free solution value until a critical interaction concentration is reached. Therefore, the hydrodynamic size of the probe is unchanged from its measured free solution value until interaction occurs. Consequently, the hydrodynamic radius of the probe can be inferred to approximate the mesh size at the interaction concentration.

Table 1. Measured Mesh Sizes in Succinylated Collagen and Hyaluronic Acid Matrices[a]

hyaluronic acid		succinylated collagen	
concn (mg/mL)	mesh size (nm)	concn (mg/mL)	mesh size (nm)
30	4 ± 0.5	43	4 ± 0.5
20	6 ± 0.5	28	6 ± 0.5
		22	11 ± 0.5

[a] The uncertainty in the mesh size is based on the uncertainty in the measured hydrodynamic radius of the probe molecules used to measure the mesh size[14] and is equal to the maximum variation between three measurements for all the probe molecules.

Table 2. Measured Mesh Sizes in Composite Matrices Containing Succinylated Collagen and Hyaluronic Acid

matrix no.	succinylated collagen (mg/mL)	HA (mg/mL)	total concn (mg/mL)	τ_R/τ_0 of R_h = 4 nm probe	τ_R/τ_0 of R_h = 6 nm probe	mesh size (nm)
1	10	20	30	1.0	0.79	4−6
2	20	10	30	1.0	0.81	4−6
3	25	5	30	1.0	0.63	4−6
4	25	15	40	0.90		<4
5	30	10	40	0.86		<4
6	20	20	40	0.88		<4
7	10	30	40	1.0	0.89	4−6

For nitroxide radicals, apparent rotational correlation times assuming quasi-isotropic motion have been calculated using the motional narrowing formalism[17,18] to be

$$\tau_R = 6.5 \times 10^{-10} w_0((h_0/h_{-1})^{0.5} + (h_0/h_{+1})^{0.5} - 2) \quad (1)$$

where h_0, h_{-1}, and h_{+1} are the peak-to-peak heights of the mid-, low-, and high-field lines in a first-derivative absorption spectrum and w_0 is the peak-to-peak line width of the mid-field line (in gauss).

The direct measurement of mesh sizes in complex mixtures, at a molecular scale, is possible with the ESR technique. The composite matrices of SC and HA were seeded with PAA mesh size probes of known size (R_h), and ESR spectra were recorded on a Varian E-4 X-band spectrometer at room temperature. The rotational correlation times of the various probes were calculated from the ESR spectra using eq 1. When the probe size approached or was greater than the matrix mesh size, the segmental dynamics of the probe were altered due to close-range interactions between the probe polymer and the matrix polymer. This change in the dynamics of the probes was detected by changes in the rotational correlation time calculated from the ESR spectra. The mesh size in the matrix was inferred to be approximately the size of the smallest probe which interacted with the matrix (i.e., the smallest probe for which τ_m/τ_0 deviated from unity, where τ_m is the rotational correlation time of the probe in the matrix and τ_0 is the rotational correlation time of the probe in free solution). This ESR-based technique provides a method for independently measuring mesh sizes in the composite matrices. Results for composite matrices of SC and HA are summarized in Table 2. The mesh sizes listed as ranges (e.g., 4−6 nm) could not be resolved more accurately because of the limited number of different size probes that were synthesized.

III. Diffusion Measurement. (a) Diffusion Probe Preparation. Bovine serum albumin (BSA) (Sigma Chemical Co., St. Louis, MO) was covalently labeled with fluorescein isothiocyanate (FITC) (Molecular Probes, Inc., Eugene, OR) in a 4% (w/w) sodium bicarbonate buffer at pH 8.4. The FITC-labeled BSA was purified by dialysis against PBS. The

Table 3. Characteristics of the Diffusing Macromolecules

macromolecule	MW (kDa)	$D_0 \times 10^7$ (cm²/s)	size (nm)
albumin (BSA)	67	5.9	13[a]
anionic dextran	69	4.5	22

[a] End-to-end length from ref 20, p 444.

removal of all unreacted FITC was verified by size exclusion chromatography. The reaction between FITC and the protein results in partial quenching of the measured fluorescence.[19] Hence, the presence of free FITC, because of unstable FITC–BSA bonds, results in increased fluorescence intensity. The stability of these probes was tested by monitoring the fluorescence of the probe solution over a period of 15 days. The fluorescence was found to remain constant over the entire period. This verified that the covalent linkage between the FITC and the protein was stable at room temperature (approximately 22 °C) over this time range. A standard calibration curve of the protein concentration vs fluorescence intensity was prepared using a fluorescence concentration analyzer (Baxter Scientific Products, Mundelein, IL). Similarly, stability of fluorescently labeled anionic dextran (Molecular Probes, Inc.), was verified and a fluorescence intensity calibration curve was prepared.

The radius of gyration (R_g) of the labeled dextran in PBS was determined by static light scattering (10–20°). The free solution diffusivity (D_0) of dextran in PBS was determined by dynamic light scattering at a scattering angle of 90°. The $\langle r^2 \rangle$ and D_0 of BSA were obtained from the literature.[20] The values for these parameters are tabulated in Table 3.

(b) Release Measurements. The diffusion experiments were performed using an "infinite-sink release-rate technique".[21] This technique was employed as opposed to more conventional diffusion measurement techniques (e.g., FRAP or LS) because the intent of these experiments was to simulate drug delivery applications. A description of the theoretical analysis of this setup is given in the following section. The matrices for the release experiments were prepared by solution mixing the matrix with a much smaller volume of labeled probe solution (much less than 0.1% w/w_{matrix}) by multiple exchanges between syringes. The mixture was then loaded into a vial and gently centrifuged to expel trapped air. The pellet which formed at the bottom of the vial (thickness ~ 1 cm) was allowed to equilibrate at room temperature for about 48 h. The release measurement was carried out at room temperature by layering 1 mL of eluting buffer (PBS) on top of the pellet. At regular intervals, the buffer was pipetted out and replaced by fresh buffer. The removal and replacement of buffer were performed without disturbing the surface of the matrix. The buffer which was removed was then assayed for the concentration of the labeled probe. The entire release experiment was performed aseptically under a laminar flow hood to prevent any bacterial contamination. This technique is shown schematically in Figure 1. Mass balances were closed at the conclusion of the release experiments by measuring the concentration of the probe remaining in the matrix through extraction of the remaining probe from the matrices by diluting and vigorously dispersing each matrix in PBS. Release measurements on each matrix composition were performed in triplicate. Under the quiescent conditions and polymer concentration range that these release experiments were performed, no swelling of the matrices was detected over the experimental time frame. The most dilute matrix concentration that was tested was limited by handling problems (i.e., loss of matrix by erosion during buffer exchange). Consequently, for HA matrices, a very limited concentration range was studied. The concentration ranges and buffer system for diffusion rate measurements were chosen to be physiologically relevant.

Data Analysis

The release of a probe (with no binding interactions present) from a monolithic matrix is governed by Fick's

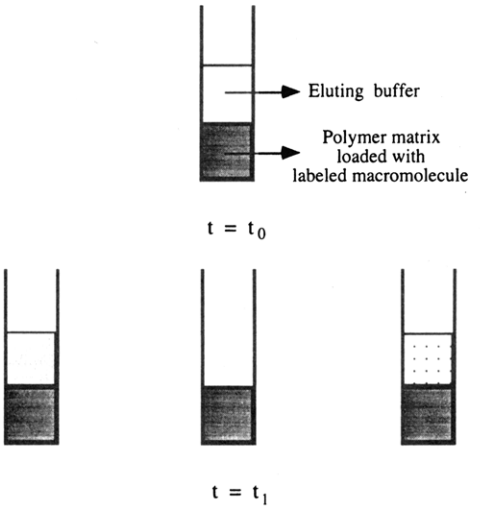

Figure 1. Experimental configuration to obtain release data of labeled probes from polymer matrices. At $t = t_0$, buffer is layered on top of the polymer matrices. At $t = t_1$, the buffer is removed and replaced by fresh buffer. The buffer which is removed is assayed for the concentration of the labeled probe that has diffused out of the matrix.

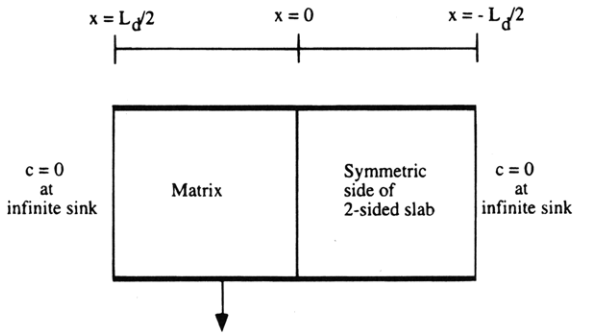

Figure 2. Schematic representation of the model matrix–infinite sink configuration used to calculate the diffusivity of the labeled probe in the polymer matrix.

second law of diffusion:[22]

$$\partial c/\partial t = \mathbf{D}\partial^2 c/\partial x^2 \tag{2}$$

where **D** is the diffusivity of the probe in the matrix, c is the concentration of the probe, t is time, and x is the length of the diffusion path. The initial and boundary conditions corresponding to the experiments can be stated by considering the release to be from one half of a two-sided slab ($L_d/2$), initially at uniform concentration (c_0), into an infinite sink (meaning that the concentration of the probe in the buffer is negligible compared to the concentration of the probe in the matrix):

$$c(t=0, x) = c_0 \tag{3}$$

$$c(t,x=L_d/2) = 0 \tag{4}$$

$$\partial c(t,x=0)/\partial x = 0 \tag{5}$$

This is schematically depicted in Figure 2. The solution of eq 2 subject to eqs 3–5 gives the time-dependent concentration profile in the matrix. The fraction of the probe remaining in the matrix ($M(t)/M_0$) at any time can be calculated by spatially integrating the concentration profile over one half of the two-sided slab:[23]

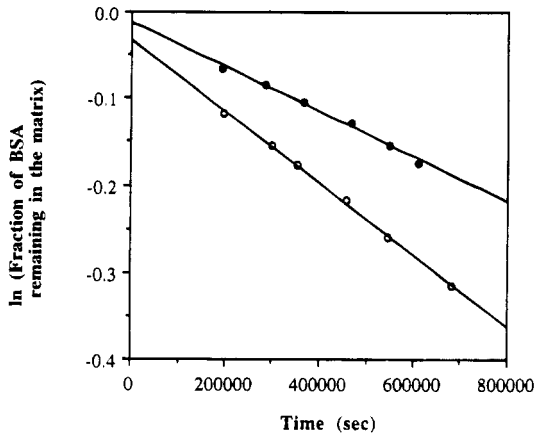

Figure 3. Plot of the log of the fraction of BSA remaining in succinylated collagen matrices vs time: (●) 40 mg/mL succinylated collagen; (○) 30 mg/mL succinylated collagen.

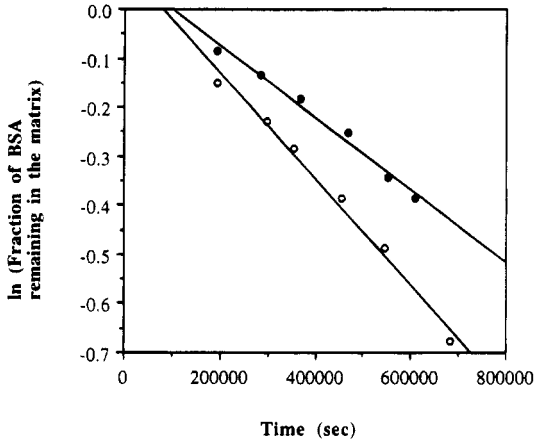

Figure 4. Plot of the log of the fraction of BSA remaining in hyaluronic acid matrices vs time: (●) 30 mg/mL hyaluronic acid; (○) 25 mg/mL hyaluronic acid.

$$M(t)/M_0 = \sum_{n=1}^{\infty} \frac{8}{n^2\pi^2}[\sin^2(n\pi/2)]\ \exp\{-(\mathbf{D}n^2\pi^2 t/L_d^2)\} \tag{6}$$

The fraction of probe released is $(1 - M(t)/M_0)$. At long times (i.e., $t \gg L_d^2/\mathbf{D}$), the $n = 1$ term in the series dominates, reducing eq 6 to

$$\lim_{t\to\infty} M(t)/M_0 = \frac{8}{\pi^2}\exp(-D\pi^2 t/L_d^2) \tag{7}$$

The solution may be assumed to be valid when the $n = 1$ term is at least 10 times greater than the next term in the series ($n = 3$). Considering the diffusivities listed in Table 3, eq 7 can be assumed to be valid for $t > 10^5$ s. Hence, based on eq 7, when the release data for $t > 10^5$ s are plotted as log[fraction remaining in the matrix] vs time, the plot should be linear and the slope would be proportional to the diffusivity of the probe in the matrix. If interactions such as probe–matrix binding or partitioning were significant, the data would deviate from linearity at $t > 10^5$ s when plotted as described above. While the release of BSA from SC followed Fickian behavior (Figure 3), the release of BSA from HA matrices showed deviations at long times (Figure 4), indicating the presence of interactions between the BSA and HA. Chemical interactions between serum proteins and glycosaminoglycans like HA have been

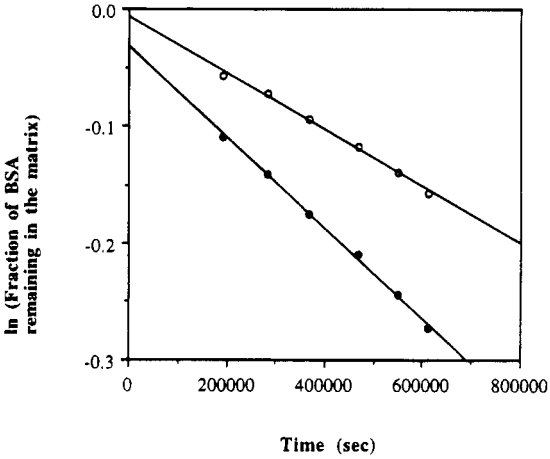

Figure 5. Plot of the log of the fraction of BSA remaining in composite matrices vs time: (●) 10 mg/mL succinylated collagen + 30 mg/mL hyaluronic acid; (○) 30 mg/mL succinylated collagen + 10 mg/mL hyaluronic acid.

reported previously.[24] These interactions retard release, and hence the analysis of the release of BSA from HA matrices by a Fickian model would tend to predict a diffusivity which is lower than the true diffusivity.[25] Despite the net negative charge on BSA, regions with a local positive charge could bind to SC. Binding experiments were performed using Centricon centrifugal filters to determine if there were nonspecific binding interactions. The molecular weight cutoff (MWCO 100K) of the filters was chosen such that the filter would selectively retain the SC. Mixtures of various ratios of SC and BSA were loaded into the Centricon filters. The concentration of SC loaded varied over a wide range and the BSA concentration was held constant. The mixtures were centrifuged till half the volume had filtered through. While the SC concentration doubled, there was no detectable increase in the concentration of BSA on the retentate side, indicating that no measurable BSA was retained due to binding between SC and BSA. The release of BSA from composite matrices of SC and HA (Figure 5) did not show deviations from Fickian behavior. This seems to indicate that the interactions between BSA and HA are weak and are suppressed in the presence of SC. Consequently, the diffusivity of BSA in HA matrices determined by a Fickian model not accounting for these weak interactions can be assumed to be an underpredicted (low) estimate of the true diffusivity. The release of anionic dextran did not show deviations from Fickian behavior at long times (not shown here), confirming that there were no appreciable binding interactions between the anionic dextran and the SC and HA matrices.

Results and Discussion

Mesh sizes in SC and HA matrices, in the concentration range studied here, have been measured previously by the ESR technique[14] and are listed in Table 1. The diffusivities of anionic dextran in SC and HA matrices were calculated using eq 7, and the values are listed in Table 4. A comparison of the diffusivities from SC and HA matrices of similar mesh sizes (Table 4) shows that the SC matrix of similar mesh size has a marginally greater retarding effect ($D/D_0 = 0.33$ in SC at 30 mg/mL and $D/D_0 = 0.35$ in HA at 30 mg/mL). Studies of the diffusion of poly(ethylene glycol) in solutions of κ-carregeenan and poly(styrenesulfonate) have shown that the stiffness of the polymer chains has an effect

Table 4. Diffusivity of Anionic Dextran in Succinylated Collagen and Hyaluronic Acid Matrices[a]

succinylated collagen (mg/mL)	hyaluronic acid (mg/mL)	mesh size (nm)	$D \times 10^7$ (cm²/s)
45		~<4	1.23 ± 0.06
40		~>4	1.35 ± 0.05
30		~<6	1.49 ± 0.01
25		6–11	1.58 ± 0.03
	30	4–6	1.57 ± 0.06

[a] ~> indicates approximately equal to but greater than and ~< indicates approximately equal to but less than. The inequalities arise because the mesh sizes were determined at polymer concentrations (Table 1) which were different from the concentrations studied here. The uncertainties in the diffusivities are based on variations between three measurements.

Table 5. Diffusivity of BSA in Succinylated Collagen and Hyaluronic Acid Matrices[a]

succinylated collagen (mg/mL)	hyaluronic acid (mg/mL)	mesh size (nm)	$D \times 10^7$ (cm²/s)
40		~>4	1.04 ± 0.01
35		4–6	1.52 ± 0.10
30		~<6	1.64 ± 0.01
25		6–11	1.86 ± 0.10
	30	4–6	3.21 ± 0.17
	25	4–6	4.52 ± 0.08

[a] The uncertainties in the diffusivities are based on variations between three measurements.

on the diffusional hindrance exerted by the matrix on the solute.[26] Predictions using Brownian dynamics simulations of diffusion of hard-sphere molecules through polymer networks of varying rigidities[27] indicate that as long as the ratio between the persistence length (p) of the matrix polymer chain and the matrix polymer radius (a), p/a, is greater than 10, the diffusional resistance encountered by the sphere is almost the same. The persistence length of the collagen molecule has been measured to be approximately 170 nm[28] and its radius is 1.5 nm (i.e., $p/a \sim 110$). The radius of the HA molecule has been calculated to be 3.7 Å[27] and its persistence length has been reported to be between 4.5 and 8.0 nm[29] (i.e., $p/a > 10$). The diffusion of anionic dextran in SC and HA matrices reported here is consistent with the predictions of the model based on diffusion of a hard sphere in a polymer network.

The diffusivity of dextran in HA (30 mg/mL) measured here ($D/D_0 = 0.35$) is in reasonable agreement but is at the high end of the range ($D/D_0 = 0.23–0.33$) predicted by the parameters used to fit the experimental data recently published by De Smedt et al.,[30] where the diffusivity of FITC-dextran ($M_w = 71.2$ kDa) in HA was measured by fluorescent recovery after photobleaching (FRAP). This is possibly because the HA employed in their experiments ($M_w = 680$ kDa) had a slightly lower molecular weight than the HA employed in these experiments and because the HA concentration used here (30 mg/mL) is outside the range (0–20 mg/mL) used to fit the data in ref 30.

The diffusivity of BSA in the same set of matrices was measured, and results are listed in Table 5. The effect of mesh size on the diffusivity of BSA is evident from the decrease in the diffusivity with decreasing mesh size. However, a comparison of the diffusivities of BSA from SC and HA matrices of similar mesh sizes shows that the SC matrices have a greater retarding effect. Previous diffusion studies[31] have shown that BSA diffuses faster in solutions of dextran ($p = 1$ nm) than in solutions of more rigid HA ($p = 4.5–8$ nm). The release of BSA from HA is not purely diffusion limited due to the weak interaction between HA and BSA. However, as discussed in the previous section, this interaction results in an underprediction of diffusivity from the analysis employed here. The measured D/D_0 of BSA in HA (0.54 at 30 mg/mL HA) appears to be a reasonable extrapolation of Ogston's[31] results for BSA diffusivites at lower HA concentrations (their data extend to an HA volume fraction of 0.004, where D/D_0 was 0.7; our experiment was at an HA volume fraction of 0.02). This suggests that the D/D_0 for BSA in HA as measured by our technique is not too high (i.e., subject to artifacts such as partitioning). Therefore we conclude that the additional diffusional hindrance produced by the SC matrix (at similar mesh sizes) is not an artifact. The increased hindrance to BSA diffusion in the SC matrices (relative to the HA matrices) is possibly due to either the greater rigidity of the SC molecules or the molecular structure of BSA. Based on X-ray crystallography data,[32] BSA is ellipsoidal with a major axis of approximately 14 nm and a minor axis of 4 nm. One can hypothesize that the behavior of BSA in rigid SC matrices is a result of coupling of rotational diffusion to translational diffusion, meaning that rotational diffusion is not unhindered as it would be for a hard sphere. Diffusion of BSA in DNA solutions has been modeled as a hard sphere diffusing through a solution of rods[33] based on the assumption that rapid rotation of BSA will effectively average over all orientations. SC used in our experiments is a more rigid polymer matrix than DNA. The mesh size in a monodisperse solution of DNA can be estimated[14] by modeling the DNA molecule as a cylindrical rod ($L = 56$ nm). The mesh sizes calculated for the DNA solutions used in their experiments (ref 33) were 8 nm at 36 mg/mL and 34 nm at 2 mg/mL. Hence, it appears that unhindered rapid rotation of BSA would be possible at the lower end of the concentration range and the rotation might be slightly hindered at higher concentrations when the mesh size was of the order of the major axis of BSA. Since the mesh sizes of the more rigid SC matrices studied here were less than 11 nm, it seems plausible that the rigid ellipsoidal geometry of BSA must be taken into account in modeling its hindered diffusion in SC matrices. In contrast, dextran, due to the conformational freedom of the α-1→6 linkages which connect the D-glucan units,[34] is more flexible and can be modeled as a hard sphere. As discussed earlier, the diffusional data for dextran in Table 4 is consistent with the hard-sphere model (D/D_0 insensitive to matrix polymer rigidity for $p/a > 10$).

Concentrated composite matrices of rod and coil polymers have not been extensively studied because of limitations in the phase stability of the two components. Previous studies of rod–coil[35] and coil–coil[36] mixtures have been restricted to lower concentration ranges due to limitations in polymer compatibility. Centrifugation of the composite matrices of SC and HA did not reveal any phase separation. Phase separation in terms of turbidity was not detected at room temperature (approximately 22 °C) for over 2 weeks. Observations of the mixtures under a polarizing microscope did not show any regions of birefringence. It is possible that at smaller size scales there may be evidence of rod anisotropy, which could be detectable with more sensitive techniques. However, the anisotropic domains would be weakly oriented and would contain a high volume

Table 6. Diffusivity of BSA in Succinylated Collagen and Hyaluronic Acid Matrices[a]

matrix no.	succinylated collagen (mg/mL)	hyaluronic acid (mg/mL)	total concn (mg/mL)	mesh size (nm)	$D \times 10^7$ (cm^2/s)
1	30		30	>~6	1.64 ± 0.01
2		30	30	4–6	3.21 ± 0.17
3	20	10	30	4–6	1.42 ± 0.03
4	10	20	30	4–6	2.00 ± 0.04
5	40		40	>~4	1.04 ± 0.01
6	30	10	40	<4	0.93 ± 0.04
7	20	20	40	<4	0.96 ± 0.04
8	10	30	40	4–6	1.45 ± 0.02

[a] The uncertainties in the diffusivities are based on variations between three measurements.

Table 7. Diffusivity of Anionic Dextran in Composite Matrices of Succinylated Collagen and Hyaluronic Acid Matrices[a]

matrix no.	succinylated collagen (mg/mL)	hyaluronic acid (mg/mL)	total concn (mg/mL)	mesh size (nm)	$D \times 10^7$ (cm^2/s)
1	30		30	>~6	1.49 ± 0.01
2		30	30	4–6	1.57 ± 0.06
3	25	5	30	4–6	1.44 ± 0.03
4	40		40	>~4	1.35 ± 0.05
5	30	10	40	<4	1.08 ± 0.02
6	25	15	40	<4	1.17 ± 0.04
7	20	20	40	<4	1.40 ± 0.04
8	10	30	40	4–6	1.60 ± 0.08

[a] The uncertainties in the diffusivities are based on variations between three measurements.

fraction of solvent.[9] The system studied here consisted of concentrated rod–coil composite matrices in which the rod submatrix mesh size was much smaller than the size of the flexible coil (coil hydrodynamic radius = 65 nm). ESR data indicating that mixing of SC and long flexible polymer chains does occur on a molecular scale will be discussed later.

Composite matrices with varying ratios of rigid and flexible polymer components were studied. A comparison of mesh sizes between SC matrices (Table 1) and composite matrices (Table 2) indicates that the addition of flexible polymer to a rigid-rod matrix yields smaller mesh sizes than can be obtained in matrices with the same total mass of rod polymer only. For example, a composite matrix of 30 mg/mL SC and 10 mg/mL HA has a smaller mesh size (<4 nm) than a matrix of 40 mg/mL SC (≥4 nm). If one envisions the composite matrix as a rigid-rod submesh with interpenetrating flexible chains, the smaller mesh sizes are a result of the flexible polymer filling in gaps in the rigid-rod submesh. Release experiments were performed with the composite matrices to study the effect of the reduced mesh sizes on diffusion. The composition of the various matrices, the measured mesh sizes, and the calculated diffusivities for BSA and anionic dextran are summarized in Tables 6 and 7, respectively. As can be seen in Table 6, the release of labeled BSA was slower in the matrices with smaller mesh sizes. The release of labeled anionic dextran from these matrices shows similar effects (Table 7). A comparison of matrices 6, 7, and 8 (Table 6) and matrices 5, 6, and 7 (Table 7) indicates that the matrices with a greater fraction of SC have a greater retarding effect than matrices with a greater fraction of HA.

To better understand the effect of the rigidity of a SC matrix on the morphology of a flexible polymer, spin-labeling studies were performed on a model linear chain polyelectrolyte whose molecular size was much larger

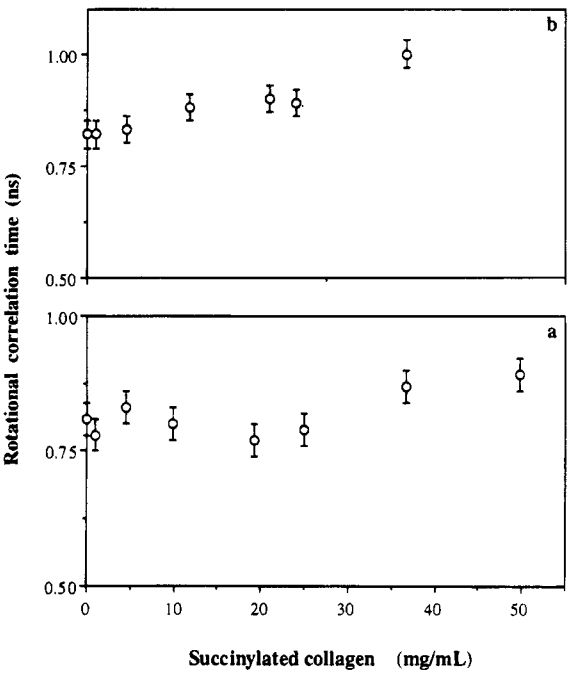

Figure 6. Rotational correlation time of PAA probe in succinylated collagen matrices. The error bars specified were determined by the maximum variation between three measurements for all the samples. (a) Probe nominal MW = 250 kDa; (b) probe nominal MW = 750 kDa.

than the SC matrix mesh size. High molecular weight linear chain poly(acrylic acid) (nominal MW 250 and 750 kDa) was labeled with the spin label 4-amino-TEMPO by the procedure described earlier to prepare PAA mesh size probes. These high molecular weight probes are termed PAA morphology probes to distinguish them from the much lower molecular weight PAA probes used in mesh size determination (termed PAA mesh size probes). The molecular weights of the PAA chains were chosen such that their sizes would be greater than the SC matrix mesh size in order to observe the distortion that is experienced by a long flexible polyelectrolyte chain (such as HA) in a SC matrix. We assume that, qualitatively, the behavior of any like charged, flexible, linear chain polyelectrolyte will be similar in a more rigid SC matrix. Thus the behavior of HA in SC matrices can be qualitatively inferred from the electron spin resonance data of spin-labeled high molecular weight PAA in SC matrices (Figure 6). The PAA morphology probes were mixed in SC matrices of various concentrations and the rotational correlation times calculated from the ESR spectra. The rotational correlation time is a measure of the time required for the nitroxide label to tumble through 1 rad of rotation about its principal axis.[37] Hence, the greater the rotational correlation time, the slower the local segmental reorientation of the polymer chain. Although the ESR spectrum directly indicates the dynamics of the spin label, for this labeling chemistry, it is reasonable to assume that it closely reflects the dynamics of the polymer backbone itself.[38] The rotational correlation times (τ_R) in free solution for both the morphology probes were found to be 0.8 ns. The lack of dependence of τ_R on the polymer molecular weight is common in large molecular weight polymers[39] since τ_R corresponds to the segmental mobility of the monomer to which the spin label is covalently bound and for very long chains the segmental mobility becomes independent of chain length. The τ_R of the probes as a function of SC

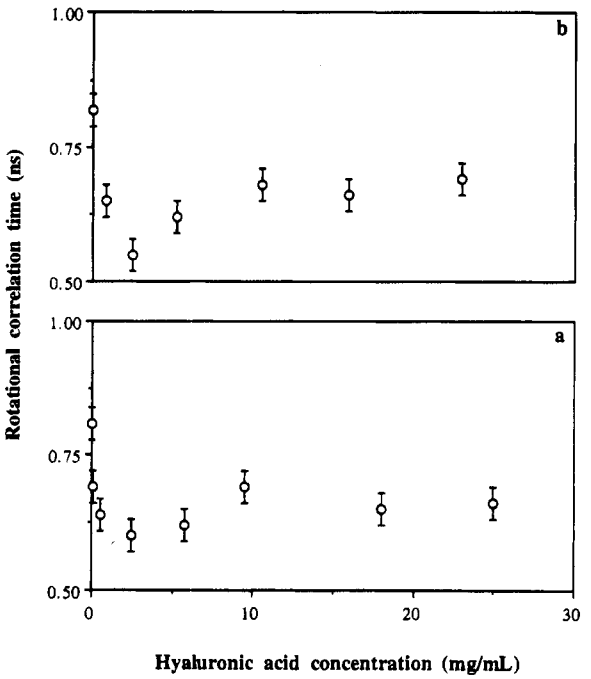

Figure 7. Rotational correlation time of PAA probe in hyaluronic acid matrices. The error bars specified were determined by the maximum variation between three measurements for all the samples. (a) Probe nominal MW = 250 kDa; (b) probe nominal MW = 750 kDa.

concentration (Figure 6) shows that the segmental mobility of the two PAA probes is unchanged at lower SC concentrations but decreases at higher concentrations. The decreased segmental mobility of the PAA probe in the SC matrices is probably a result of the ability of the rigid SC molecule to interpenetrate the flexible chain at higher SC concentrations. The critical SC concentration at which the network interpenetrates the flexible coil is approximately 20 mg/mL for the 250 kDa PAA (Figure 6a) and about 5 mg/mL for the 750 kDa PAA (Figure 6b). The decreased segmental mobility of the probe in the SC matrices at higher collagen concentrations implies rigidification of the flexible chain. It has been suggested recently[35] that a linear random coil polymer surrounded by rodlike polymers would favor conformations that run nominally straight over length scales comparable to the correlation length of the rods. This linearly correlated conformation could account for the reduced segmental mobility of the flexible polymer. Hence, it appears that composite matrices with a greater SC content possess greater rigidity not only because of the larger rod content itself but also because of the influence of the rod content on the morphology of the flexible polymer.

The morphology probes were also added to HA matrices of various concentrations. The lower τ_R of the PAA probes in the hyaluronic acid matrices (Figure 7) compared to free solution is presumably due to the contraction of linear random coil polymers in the presence of the other linear random coil polymers.[40] At higher HA concentrations, unlike SC, the τ_R in the HA matrices (Figure 7) indicates that the segmental mobility is essentially unchanged (the hard-sphere limit) with increasing HA concentration.

A comparison of the diffusivity of dextran in matrices 5, 6, and 7 (Table 7) indicates increased diffusional hindrance with increasing SC content. Since both SC and HA are relatively rigid ($p/a > 10$), the effect of the increased rigidity of HA on the diffusional behavior of dextran in the composite matrix is probably small. Hence, it is reasonable to interpret the increased hindrance in matrix 5 (Table 7) to be due to a smaller mesh size than in matrices 6 and 7 (Table 7) (mesh sizes which could not be resolved by the ESR measurements). The difference in the diffusional hindrance of BSA in matrices 2, 3, and 4 (Table 6) cannot be attributed to decreased mesh size alone since the increased rigidity of HA with higher SC fractions could also impact the diffusional behavior of BSA (due to rotational–translational diffusion coupling).

Conclusions

Diffusion of macromolecules in matrices of SC (a rigid rod) and HA (a flexible coil) was studied. The diffusional behavior of ellipsoidal solutes in these polymer matrices is influenced by both mesh size and polymer chain rigidity. In particular, with BSA in concentrated SC matrices, rotational and translational diffusion appear to become coupled. ESR studies of the morphology of a flexible polymer in the presence of rigid SC chains indicate that the two chains mix and that the flexible-chain rigidity increases. Furthermore, the apparent interpenetration of long-chain flexible molecules within a rigid-rod matrix submesh reduces the overall composite matrix mesh size. The extent to which the decreased diffusion rates of ellipsoidal polymer solutes in these composite matrices are a consequence of the reduced mesh size or enhanced flexible component chain rigidity remains to be conclusively determined.

Acknowledgment. We thank Dr. A. K. Gaigalas for his assistance with the light scattering measurements. We also thank the reviewers for their helpful comments.

References and Notes

(1) Langer, R. *Science* **1990**, *249*, 1527.
(2) Hutchinson, F. G.; Furr, B. J. A. *J. Controlled Release* **1990**, *13*, 279.
(3) Pitt, C. G. *Int. J. Pharm.* **1990**, *59*, 173.
(4) Pachence, J. M.; Berg, R. A.; Silver, F. H. *Med. Device Diagn. Ind.* **1987**, 49.
(5) Balazs, E. A.; Band, P. *Cosmet. Toiletries* **1984**, *99*, 65.
(6) Piez, K. A. In *Encyclopedia of Polymer Science and Engineering*; Wiley: New York, 1985; Vol. 3.
(7) Piez, K. A. In *Extracellular Matrix Biochemistry*; Piez, K. A., Reddi, A. H., Eds.; American Elsevier Science Publishing Co.: New York, 1984; p 1.
(8) Flory, P. J. *Macromolecules* **1978**, *11*, 1138.
(9) Flory, P. J. *Proc. R. Soc. London, A* **1956**, *234*, 73.
(10) Doi, M.; Edwards, S. F. *The Theory of Polymer Dynamics*; Clarendon Press: Oxford, 1986.
(11) Miyata, T.; Rubin, A. L.; Stenzel, K. H.; Dunn, M. W. Collagen Drug Delivery Device. U.S. Patent No. 4,164,559, 1979.
(12) Gornall, A. G.; Bardawil, C. J.; David, M. M. *J. Biol. Chem.* **1949**, *177*, 751.
(13) Shah, C. B.; Barnett, S. M. In *Polyelectrolyte Gels*; Harland, R. S., Prud'homme, R. K., Eds.; ACS Symposium Series 480; American Chemical Society: Washington, DC, 1992; p 116.
(14) Shenoy, V.; Rosenblatt, J.; Vincent, J.; Gaigalas, A. *Macromolecules* **1995**, *28*, 527.
(15) Wielema, T. A.; Engberts, J. B. F. N. *Eur. Polym. J.* **1988**, *24*, 647.
(16) Buchachenko, A. L.; Kovarskii, A. L.; Wassermann, A. M. In *Study of Polymers by Paramagnetic Probe Methods*; Rogovin, Z. A., Ed.; Halsted Press: New York, 1976; p 26.
(17) Freed, J. H.; Fraenkel, G. K. *J. Chem. Phys.* **1963**, *39*, 326.
(18) McConnell, H. M. *J. Chem. Phys.* **1956**, *25*, 709.
(19) Haugland, R. *Handbook of Fluorescent Probes and Research Chemicals*, 5th ed.; Molecular Probes, Inc.: Eugene, OR, 1992.
(20) Tanford, C. *Physical Chemistry of Macromolecules*; Wiley: New York, 1961.
(21) Rosenblatt, J.; Rhee, W.; Wallace, D. *J. Controlled Release* **1989**, *9*, 195.

(22) Crank, J. *The Mathematics of Diffusion*; Oxford University Press: Oxford, 1975.
(23) Baker, R. W.; Lonsdale, H. K. In *Controlled Release of Biologically Active Agents*; Tanqueray, A. C., Lacey, R. E., Eds.; Plenum: New York, 1974.
(24) Underhill, C. B. *Biochem. Biophys. Res. Commun.* **1982**, *108*, 1488.
(25) Desai, S. J.; Singh, P.; Simonelle, A. P.; Higuchi, W. F. *J. Pharm. Sci.* **1966**, *55*, 1224.
(26) Johannson, L.; Skantze, U.; Lofroth, J. *Macromolecules* **1991**, *24*, 6019.
(27) Johannson, L.; elvingson, C.; Lofroth, J. *Macromolecules* **1991**, *24*, 6024.
(28) Nestler, F. H. M.; Hvidt, S.; Ferry, J. D.; Veis, A. *Biopolymers* **1983**, *22*, 1747.
(29) Fouissac, E.; Milas, M.; Rinaudo, M.; Borsali, R. *Macromolecules* **1992**, *25*, 5613.
(30) De Smedt, S. C.; Lauwers, A.; Demeester, J.; Engelborghs, Y.; De Mey, G.; Du, M. *Macromolecules* **1994**, *27*, 141.
(31) Ogston, A. G.; Preston, B. N.; Wells, J. D. *Proc. R. Soc. London, A* **1973**, *333*, 297.
(32) Squire, P. G.; Moser, P.; O'Konski, C. T. *Biochemistry* **1968**, *7*, 4261.
(33) Wattenbarger, M. R.; Bloomfield, V. A.; Bu, Z.; Russo, P. S. *Macromolecules* **1992**, *25*, 5263.
(34) Brant, D. A.; Burton, B. A. In *Solution Properties of Polysaccharides*; American Chemical Society: Washington, DC, 1981.
(35) Jamil, T.; Russo, P. S.; Negulescu, I.; Daly, W. H.; Schaefer, D. W.; Beaucage, G. *Macromolecules* **1994**, *27*, 171.
(36) Kent, M. S.; Tirrell, M.; Lodge, T. P. *Macromolecules* **1992**, *25*, 5383.
(37) Carrington, A.; McLachlan, A. D. *Introduction to Magnetic Resonance*; Harper: New York, 1967.
(38) Bullock, A. T.; Cameroon, G. G. In *Structural Studies of Macromolecules by Spectrophotometric Methods*; Ivin, K. J., Ed.; Wiley: New York, 1976; p 273.
(39) Miller, W. G. In *Spin Labeling, Theory and Applications*; Berliner, L. J., Ed.; Academic Press: New York, 1979; Vol. 2, p 173.
(40) Daoud, M.; Cotton, J. P.; Farnoux, B.; Jannink, G.; Sarma, G.; Benoit, H.; Duplessix, R.; Picot, C.; de Gennes, P.-G. *Macromolecules* **1975**, *8*, 804.

MA946416C